

Laser beam scattering effects in non-absorbent inhomogeneous polymers

Mariana Ilie^{a,b}, Jean-Christophe Kneip^b, Simone Mattei^{b,*}, Alexandru Nichici^a,
Claude Roze^c, Thierry Girasole^c

^aPolitehnica University of Timisoara, Mihai Viteazu nr.1, Timisoara 300222, Romania

^bLaboratoire Laser et Traitement des matériaux, IUT Le Creusot, Université de Bourgogne, 12 rue de la Fonderie, 71200, Le Creusot, France

^cCORIA, UMR 6614, CNRS—Université et INSA de Rouen, Site Universitaire du Madrillet, BP 12, 76801, Saint-Etienne du Rouvray, France

Received 14 March 2006; accepted 18 July 2006

Available online 6 October 2006

Abstract

In this paper a numerical model for laser beam scattering in the semi-transparent polymers is presented, using a Monte Carlo algorithm and the Mie theory. The algorithm correctly accounts for the independent multiply-scattered light. We describe the algorithm, present a number of important parameters that account in the welding process, and explicitly show how the algorithm can be used to estimate the laser beam intensity both inside the semi-transparent component and at the welding interface and the beam widening. For the model validation an experimental bench test has been realized and some results from two test cases are presented.

© 2006 Elsevier Ltd. All rights reserved.

Keywords: Laser welding; Light scattering; Polymer; Mie theory; Monte Carlo

1. Introduction

As known, the thermoplastics laser welding is a modern and innovative technology with well-known general advantages of laser materials processing, as a non-contact, non-contaminant process, flexible, easy to control and automate. A better knowledge of the scattering phenomena and their importance in the polymers welding process are imperatively required due to the fast and continuous development in this area and to the large variety of thermoplastics family.

During the last decade, the research on this subject has recorded a great development, regarding new laser sources, new absorbers, increasing speed, mathematical modeling and industrial applications. Still the current level of laser welding technology is far from maturity and researchers and manufacturers alike are actively seeking new methods of understanding and optimizing the process.

In essence, through-transmission laser welding requires an optically transparent part and an absorbing one and a preferential deposition of energy in order to melt the

material in the interfacial zone. The process efficiency is strongly dependent on the optical properties of the two parts to be welded (reflectance, transmittance and absorbance) so it is very important to quantify the influence of each of these on the beam attenuation.

Since the real polymeric materials contain a large variety of heterogeneities (mineral filler, additives, pigments...), the energy deposition at the welding interface may be dramatically reduced and subsequently affect the welding potential.

Generally, an electromagnetic wave traveling through a medium is attenuated by an extinction phenomenon, in which absorption and scattering effects can equally coexist or prevail to each other. In the present study, we will consider only non-absorbent inhomogeneous mediums in order to quantify the scattering effects.

The final goal in our study is to predict the thermoplastics weldability by determining the thermal field developed inside the components to be joined and the structure behavior under laser irradiation. The first task in pursuit of this goal is to quantify the beam attenuation in the semi-transparent polymers by making connection between the optical properties of the bulk materials of which the heterogeneities and the medium are made and

*Corresponding author. Tel.: +33 85 73 10 42; fax: +33 85 73 11 20.

E-mail address: s.mattei@iutlecreusot.u-bourgogne.fr (S. Mattei).

the laser intensity spatial distribution into the medium. The second is to utilize these results for further numerical simulation of the welding process with a FEM-based code.

In order to accomplish the first task we used a hybrid code developed by the CORIA laboratory and slightly modified to fit in with the exact experimental conditions. The code combines the accuracy advantages of Mie theory and Monte Carlo simulation in a hypothesis of an incoherent scattering.

2. Theoretical consideration

2.1. Scattering theory

The exact analytical solution of Maxwell’s equations for the scattering of an electromagnetic plane wave from a spherical, homogenous particle is given by Mie theory since 1908 [1]. During the last years, intensive efforts have been devoted to overcome the limitations of this theory and generalize it to different laser beams profiles and asymmetric shapes of scatters [2–4].

Considering the case of a single particle, the Mie theory provides the scattering parameters which offer us the first information on how efficient the particle will scatter the radiation, that is: scattering cross-section C_{sca} , absorption cross-section C_{abs} and phase function $p(\theta)$. Anisotropy factor g may then be deduced. We will briefly explain each of them, more detailed information can be found in [5,6].

The scattering cross-section gives the probability of photon scattering per unit path-length and multiplied by the particles concentration n is the reciprocal to the mean free path $l_{sca} = 1/n \cdot C_{sca}$ (the average distance traveled by the photon between two successive scattering events).

This parameter is a very important one in establishing if there is a simple or a multiple scattering regime. For a medium with a thickness $L \approx l_{sca}$ the photons will be scattered once, which simplifies the issue because there is a proportionality relationship between the scattered intensities (the scattered intensity by the medium is N times that scattered by a single particle).

For higher volume fractions, where $l_{sca} \ll L$, the scattering regime is a multiple one, and it is a more complex case especially when we deal with the dependent scattering regime. Dependent scattering denotes scattering process where the mechanism of particle–wave interaction itself is modified by the presence of neighboring particles [7]. Generally, assuming a random distribution of scatters can make considerable simplifications. This brings us to the incoherent scattering case but it is difficult to state precise general conditions under which this scattering criterion is satisfied.

In addition to these angle-independent quantities, Mie theory allows us to calculate the angular distribution of the scattered radiation in the far-field of the particle. The amount of the scattered radiation into a solid angle about a given direction is the differential cross-section $dC_{sca}/d\Omega$ and the angular distribution is usually expressed in terms of

the angular distribution function $p(\cos \theta)$ known as the phase function in the light scattering literature:

$$p(\cos \theta) = \frac{1}{k^2 C_{sca}} \frac{dC_{sca}}{d\Omega}, \tag{1}$$

where $k = 2\pi/\lambda$ is the wave number, with λ the wavelength of light in the medium.

The anisotropy factor is an averaged cosine of the scattered angle and it can take values close to -1 for a backscattering, 1 for a forward scattering and 0 for an isotropic scattering (Fig. 1).

2.2. Monte Carlo algorithm

After obtaining the scattering parameters mentioned above from Mie theory, we apply the Monte Carlo method widely used in multiple scattering topic [8,9], in which the trajectories of light rays (commonly called “photons”) are simulated probabilistically through the considered medium until they hit a predefined detecting area. We present a flowchart in Fig. 2 that illustrates the main steps in Monte Carlo technique.

2.2.1. Photon initialization

In this study, a plane–parallel medium, infinite in the x and y -directions, with a thickness L in the z -direction, containing random distributed, identically sized, non-absorbing spheres and illuminated by a Gaussian collimated beam in normal incidence is considered. Radius of the beam is assumed to be larger that the diameter of the particles.

When the photons are launched, their initial position (defined by radius r and angle ϕ) inside the beam section is chosen. Angle ϕ is equidistributed inside $[0, 2\pi]$ and radius

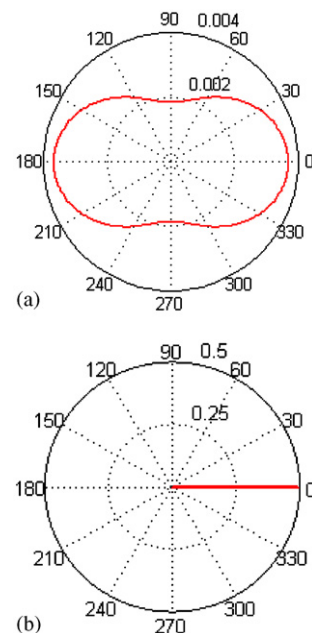


Fig. 1. Phase function for $g = 0.06$ (a), $g = 0.96$ (b).

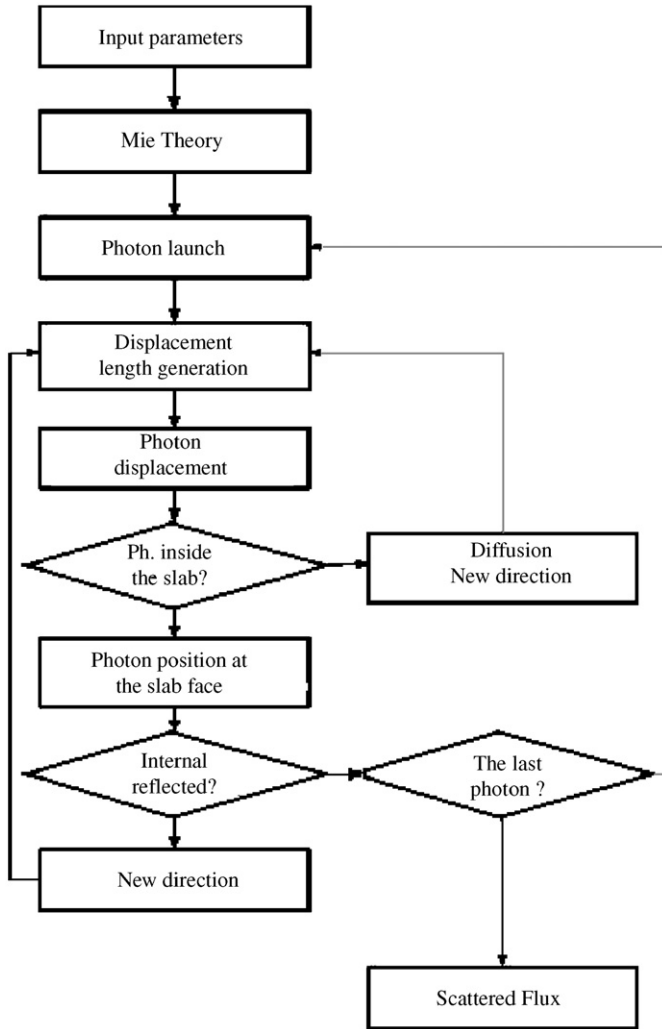


Fig. 2. Flowchart for the Monte Carlo method.

r is drawn accordingly to a Gaussian distribution. The initial direction for propagation is chosen downward into the scattering medium. So, once the radius r and the angle ϕ are chosen, the initial position of the photon is generated, resulting a photon position on the first side of the slab specified by the Cartesian coordinates:

$$\begin{cases} x = r \cos(\phi), \\ y = r \sin(\phi), \\ z = 0. \end{cases} \quad (2)$$

From this position, the photon is inserted orthogonally into the slab by setting the directional cosines to $(0,0,1)$.

2.2.2. Photon propagation

To simulate propagation, Monte Carlo method chooses a distance for collision of the photon with a particle. The photon step size is calculated based on a sampling of the probability distribution for photon's mean free path $l_{\text{ext}} = -\ln(\xi)/k_{\text{ext}}$, $l_{\text{ext}} \in [0, \infty]$, where ξ is a random variable uniformly distributed over the interval $[0,1]$ and

$k_{\text{ext}} = k_{\text{abs}} + k_{\text{sca}} = k_{\text{sca}} = n \cdot C_{\text{sca}}$, where k_{ext} is the total attenuation (extinction), k_{sca} the absorption coefficient, k_{abs} the scattering coefficient and n the particle concentration.

2.2.3. Photon scattering

Once the photon hits a particle, it is scattered because the particle is non-absorbent. The scattering direction is chosen according to the normalized phase function provided by Mie theory, which describes the probability density function for the azimuthal and longitudinal angles.

Scattering direction is defined by two angles (θ, φ) relatively to the incident direction. Since we consider an unpolarized radiation and spherical particles, the phase function has no azimuthally dependence, so angle φ is uniformly distributed between 0 and 2π :

$$\varphi = 2\pi\xi,$$

where ξ is a pseudo-random number uniformly distributed over interval $[0,1]$.

Angle θ is chosen using the phase function, given a pseudo-random number, by inverting the following integral:

$$\xi = \frac{\int_0^\theta p(\theta) \sin(\theta) d\theta}{\int_0^\pi p(\theta) \sin(\theta) d\theta}. \quad (3)$$

Once the deflection angle θ and the azimuthal angle φ are chosen, the new direction for the photon propagation can be calculated using the next formulas [10]:

$$\begin{aligned} k'_x &= \frac{\sin(\theta)}{\sqrt{1-k_z^2}} \cdot (k_x \cdot k_z \cdot \cos(\varphi) - k_y \cdot \sin(\varphi)) + k_x \cdot \cos(\theta), \\ k'_y &= \frac{\sin(\theta)}{\sqrt{1-k_z^2}} \cdot (k_y \cdot k_z \cdot \cos(\varphi) + k_x \cdot \sin(\varphi)) + k_y \cdot \cos(\theta), \\ k'_z &= -\sin(\theta) \cdot \cos(\varphi) \cdot \sqrt{1-k_z^2} + k_z \cdot \cos(\theta). \end{aligned} \quad (4)$$

The direction cosines $k_{\{x,y,z\}}$ are the cosines of the angle that the photon's direction makes with each axis in the slab referential.

If the photon is moving over the z -direction, use of the above formulas will lead to a division by zero, since $k_z = 1$, so for avoiding this the following formulas have to be used:

$$\begin{aligned} k'_x &= \sin(\theta) \cdot \cos(\varphi), \\ k'_y &= \sin(\theta) \cdot \sin(\varphi), \\ k'_z &= \text{sign}(k_z) \cdot \cos(\varphi). \end{aligned} \quad (5)$$

2.2.4. Reflection or transmission at the boundary

Since the photons are traveling in a plane-parallel medium, it is necessary to take into account the possibilities of internal reflection on the upper and lower boundaries of the medium. Consequently, the probability of a photon being internally reflected is computed according to the

Fresnel reflection coefficient $R(\theta_i)$:

$$R(\theta_i) = \frac{1}{2} \left[\frac{\sin^2(\theta_i - \theta_t)}{\sin^2(\theta_i + \theta_t)} + \frac{\tan^2(\theta_i - \theta_t)}{\tan^2(\theta_i + \theta_t)} \right], \quad (6)$$

where $\theta_i = \cos^{-1}(|k_z|)$ is the angle of incidence at the boundary and θ_t is given by the Snell's law $n_i \sin \theta_i = n_t \sin \theta_t$.

By comparing the internal reflectance $R(\theta_i)$ with a random number ξ , it is determined whether the photon is internally reflected or transmitted:

- for $\xi > R(\theta_i)$ the photon escapes the slab and it is recorded by the detector as the transmitted radiation when it leaves at the bottom or a backscattered one when it leaves at the top,
- for $\xi \leq R(\theta_i)$ the photon is internally reflected and its directional cosines are updated by reversing the z component.

Absorption from neither the host medium nor the dispersed phase has been considered in this study, even if it is already implemented in the code. As we restricted ourselves to mono-sized scattering particles, no size averaging has been implemented.

Following all this numerical computation, we obtain the profile of the laser beam distribution both inside and at the exit of the slab.

3. Numerical simulation

The scenario for our numerical simulations involves a homogenous, non-absorbent matrix with a value for refractive index of 1.49, a 0.001 volume fraction of scattering particles with diameters ranging from 0.02 to 100 μm (in 0.02 μm increments), with refractive index lower or greater than that of the matrix, and a NIR incident radiation with a 808 nm wavelength.

Since the incident beam is generated with a Gaussian distribution of the intensity and the transmitted ones preserve the same distribution (Fig. 3), as criterion for comparison between them we choose two parameters: on axis intensity and the $1/e$ radius.

The results of this scenario are provided in Fig. 4 up to a particle diameter of 5 μm for sake of data clarity (Fig. 4):

Analyzing the evolution of the transmitted beam, we notice a greater scattering efficiency and dependency on particle size for stronger relative refractive index. We can easily delimit three intervals with different “scattering” behaviors. For the particles smaller than $\lambda/10$ the medium is nearly homogenous from the optical point of view. This originates in the fact that in this interval the scattering cross-section C_{sca} has extremely small values so the mean free-path l_{sca} is becoming quite large (the light does not see the particles). For the particles with a diameter greater than 20λ , in the scattering pattern the most important contribution belongs to the diffraction phenomena. The angular

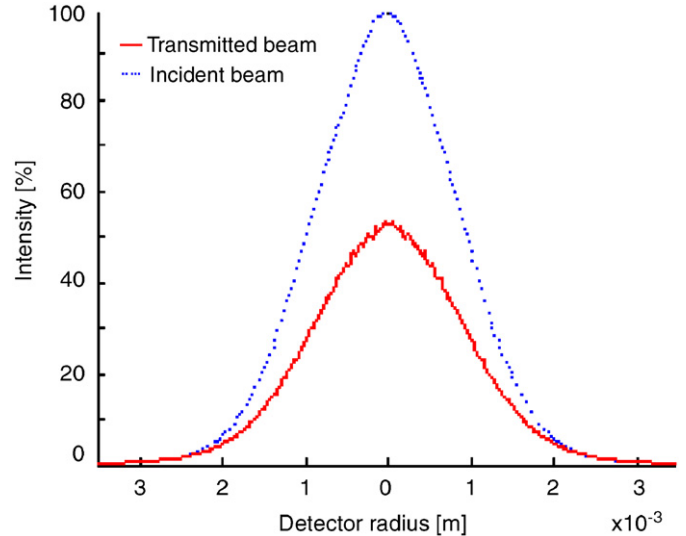


Fig. 3. Gaussian distribution of the intensity for the incident and the transmitted beam for a 2 mm sample charged with particles of 0.297 μm diameter and a volume fraction $f = 0.001$.

distribution of the scattered radiation is strongly peaked in forward direction, confining the scattering directions to smaller angles.

When the particle diameter is comparable to the wavelength the beam scattering can be important. The evolution of the radius shows significant beam dispersion for values of particle diameter around $\lambda/2$, together with intensity attenuation which can attain 15% of incident value. This domain is known as Mie resonance [10]. The maximum has a tendency to shift to smaller values of particle diameter as the ratio between the particle and the host refractive index n_p/n_h is increasing (e.g. from 0.54 μm at $n_p = 1.7$ to 0.44 μm at $n_p = 1.9$).

A closer image of the “scattering reasons” is obtained if we take into account all the contributing factors to the process. If we “compress” all the particles into a homogenous slab (fraction volume $f = 1$) without losing their identities and properties, we have the first representation about how efficient a fixed mass of particles is in removing light from a beam. This information is given by the volume attenuation coefficient expressed in absence of absorption as C_{sca}/v where v is the particle volume [7]. In the next two plots (Fig. 5), we represent the theoretical evolution of the volume attenuation coefficient as a function of particle diameter for different particle refractive index.

Once again, the trend in greater scattering efficiency and dependency on particle size for stronger relative refractive index is obvious. It is interesting to observe that the particle diameter range that covers the maxima of these curves is much larger than that of maxima for transmitted beam radius. This clearly implies a slightly different behavior of a medium containing randomly distributed scatters from a bulk one mentioned above. If we consider a particle refractive index $n_p = 1.8$ (which gives a relative refractive

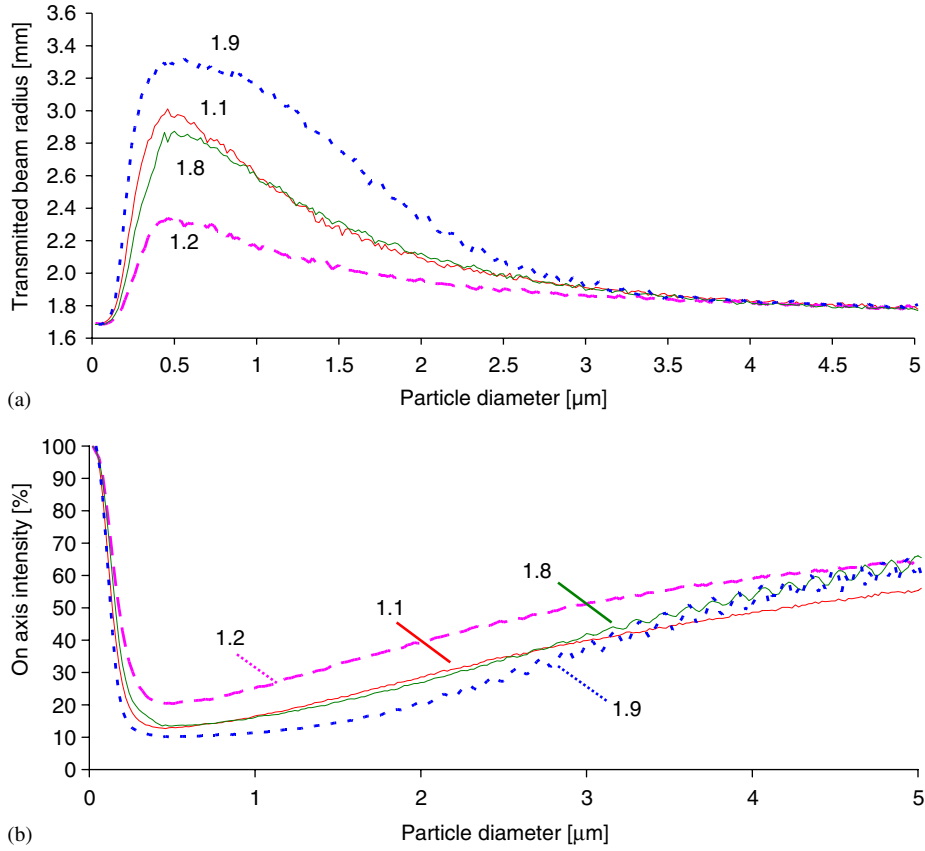


Fig. 4. Evolution of $1/e$ radius (a) and on axis intensity (b) for the transmitted beam as function of particle diameter.

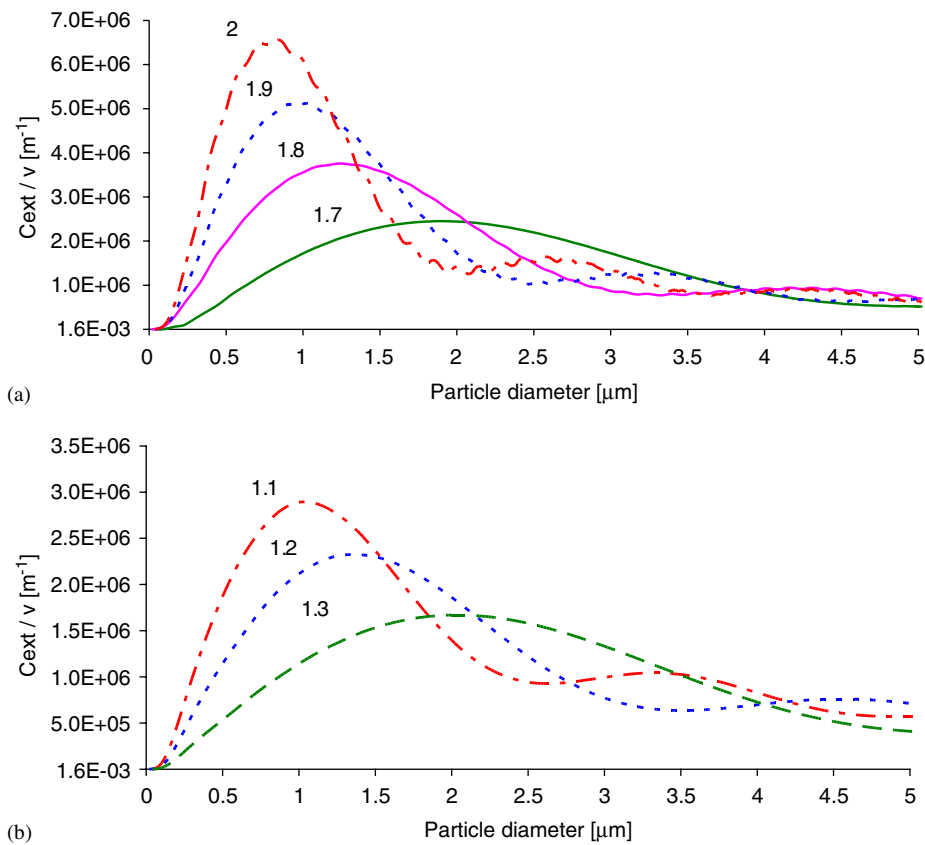


Fig. 5. Volume attenuation coefficient C_{sca}/v for particles with refractive index greater (a) and lower (b) than matrix index ($n_h = 1.49$) as function of particle diameter for a volume fraction $f = 0.001$.

index $n = 1.2$), the maximum of the volume attenuation coefficient occurs for $d = 1.24 \mu\text{m}$ but the maximum for transmitted beam radius is shifted to $d = 0.5 \mu\text{m}$. This

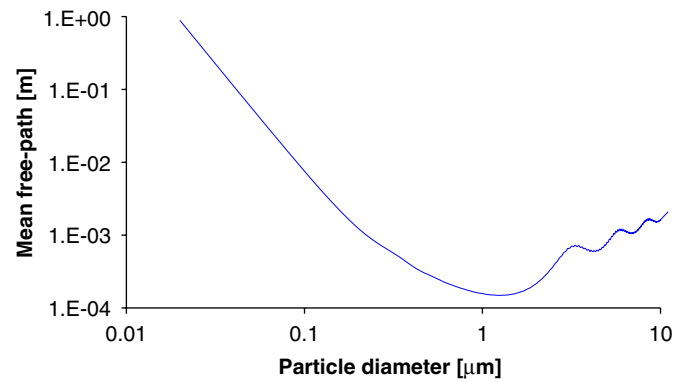


Fig. 6. Evolution of mean free-path as a function of particle diameter for $n_p = 1.8$, $n_h = 1.49$ and a volume fraction $f = 0.001$.

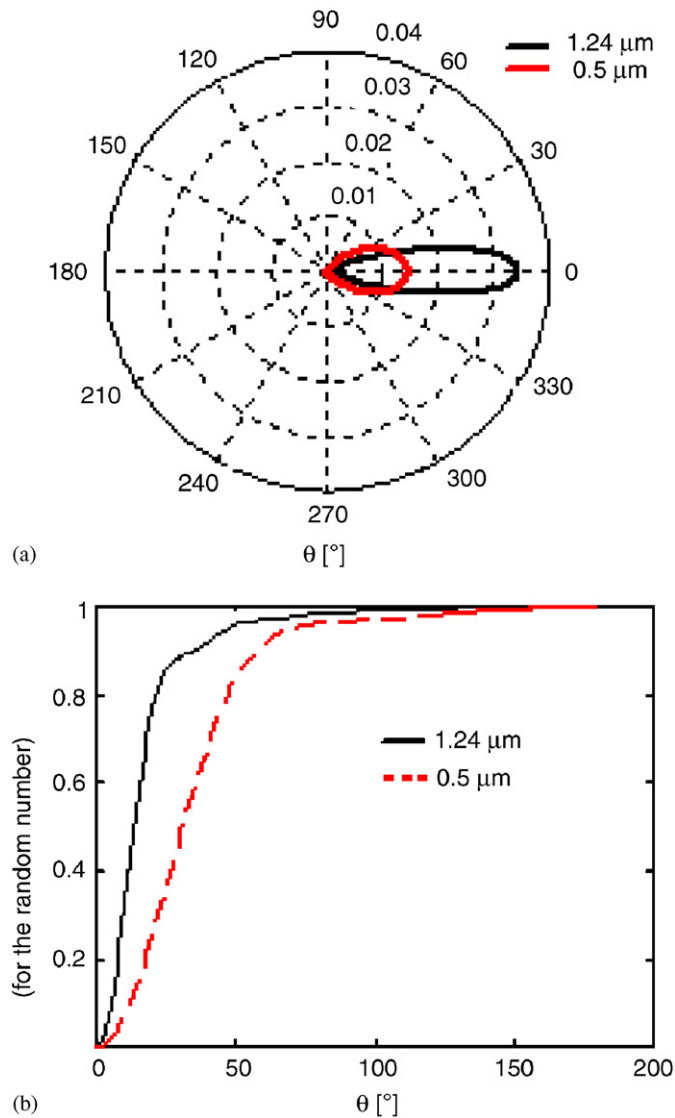


Fig. 7. Phase function (a) and the density probability function path (b) for two particle diameters $d = 0.5$ and $1.24 \mu\text{m}$.

difference might seem intriguing since an analysis of a mean free-path evolution indicates the same particle diameter as the most effective scatterer as the volume attenuation coefficient (Fig. 6).

The decisive parameter for this situation is the phase function. If we represent it (Fig. 7) for the two considered maxima, 0.5 and $1.24 \mu\text{m}$, and estimate the probability density for the scattering direction it becomes quite clear why a medium containing particles with $0.5 \mu\text{m}$ diameter is more effective in spreading out the laser beam. Every scattering event for a photon in a medium with $0.5 \mu\text{m}$ particles means a new traveling direction described by a scattering angle between 0 and 50 degrees since for the $1.24 \mu\text{m}$ particles the scattering angle is limited to 0 – 20 so the latter case is a more forward scattering one.

Perceiving the complexity of the issue it is desirable to integrate these factors in a more global parameter in order to facilitate the characterization of the optical properties of a medium.

Using the developed code, we are also able to model the profile of the laser beam both inside and at the exit of the slab. We use a non-linear regression approximation for the $1/e$ transmitted beam radius and on axis intensities as can be seen in Fig. 8.

Utilizing this results in a finite element method based program we will be able to investigate the possibility of

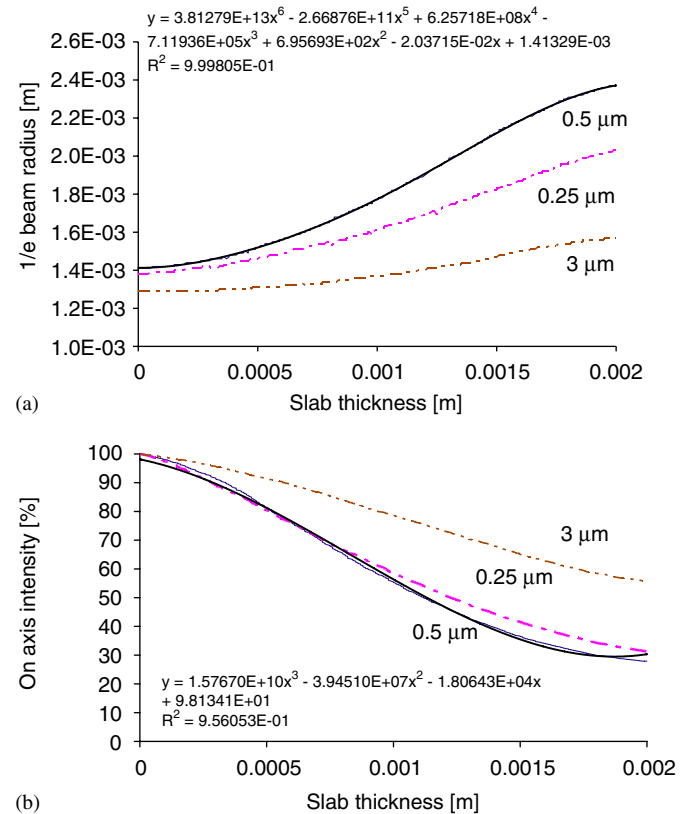


Fig. 8. Evolution of $1/e$ beam radius (a) and on axis intensities (b) within a 2 mm slab thickness and the three particle diameters indicated on the curves simulated for $n_p = 1.8$, $n_h = 1.49$, $f = 0.001$. An example for a non-linear approximation is represented on the $0.5 \mu\text{m}$ curve.

welding of different types of polymers and to establish from the beginning the suitable parameters for the welding process.

Such knowledge can lead to an important reduction of the experimental time and concentrate the efforts in optimizing the process rather than realizing it.

4. Experimental

In order to validate the numerical model used for simulating the laser scattering in a plane-parallel medium containing scattering particles an experimental bench has been constructed (Fig. 9). A diode laser with 808 nm wavelength with optical components is used to obtain a collimated beam with a $1/e$ radius of 1.12 mm. The sample is fixed into laser beam path and the transmitted beam profile is obtained by means of a linear light intensity to voltage converter type with an active area of 0.26 mm^2 connected to a data acquisition system. For a complete characterization of the beam, two micrometric tables (Table X and Table Y) are used to allow the sensor motion on two orthogonal directions.

The samples were prepared by charging an amorphous matrix of PMMA with different sized silica particles with two concentrations C provided by DEGUSSA. The PMMA slab thickness is 3 mm for all the resulting samples.

As it is shown in Table 1, all the measurements made on the samples charged with small particles, 0.007 and $0.04 \mu\text{m}$, demonstrate as we expected that in that area the

medium is homogenous from the optical point of view so the recorded transmitted beam is identical with the incident one. The incident $1/e$ beam radius is 1.12 mm.

For the samples charged with 5.5 and $7 \mu\text{m}$ silica particles at the concentrations mentioned above, the experimentally measured $1/e$ radii of the transmitted beam begin to show a dispersion effect.

Having a complex refractive index $n = 1.432 - 3 \times 10^{-5}i$ at 800 nm, the fused silica shows no absorption at this wavelength so all the dispersal effects are due only to the beam scattering inside the samples. We identify a descending trend of the scattered beam radius as we pass to a bigger particle diameter, as it was recorded in the numerical study of the scattering phenomena described in the previous paragraph. As we increase the particles concentration the beam widening becomes more important.

5. Conclusion

Using a hybrid code, which combines the Mie theory and the Monte Carlo method, we have studied the scattering phenomena in semi-transparent polymers in absence of absorption. We identified the cases for which the medium remains homogenous from the optical point of view no matter the particles concentration. We also saw that particles with diameters comparable to the wavelength can induce an important attenuation of the laser beam. This will be more pronounced as we increase the particles fraction volume, the sample thickness or the relative refractive index.

The numerical computations allowed us to obtain the profile of the laser beam distribution both inside and at the exit of the slab. The result can be used to define the heat source profile and its magnitude required for further numerical simulations of the welding process using finite element method, in order to predict materials weldability. It will allow an efficient prediction of the weld quality for a range of laser speeds and powers on different plastics thus reducing the experimental time and concentrating the efforts in optimizing the process.

Experimentally measures made on PMMA samples charged with different sized silica particles at two concentrations confirmed our modeling results.

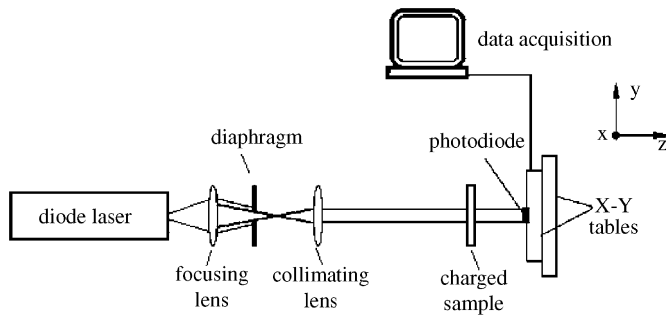


Fig. 9. Experimental bench for measuring the transmitted beam through the scattering media.

Table 1
The experimentally measured intensities and $1/e$ beam radii transmitted through the charged samples

Theories	Silica	D (μm)	C (%)	Measured $1/e$ radius (mm)	Simulated $1/e$ radius (mm)	Deviation (%)	Measured intensity (%)	Simulated intensity (%)	Deviation (%)
Rayleigh	Aerosil	0.007	2.5	1.12	1.12	0	95	96	1
	300	0.007	5	1.12	1.12	0	90	96	6
Domain	Aerosil	0.04	2.5	1.12	1.12	0	95	96	1
	OX 50	0.04	5	1.12	1.12	0	90	96	6
Mie	Sipernat	5.5	2.38	1.37	1.38	1	78	83	5
	310	5.5	4.75	1.4	1.47	7	65	67	2
Domain	Sipernat	7	1.97	1.31	1.32	1	83	90	7
	20	7	3.9	1.34	1.39	5	74	79	5

Acknowledgments

We would like to thank the industrial partners DE-GUSSA for providing materials and advices.

References

- [1] Mie G. Beiträge zur Optik trüber Medien, speziell kolloidaler Metallösungen. *Ann Phys* 1908;25:377.
- [2] Gouesbet G, Gréhan G. Generalized Lorenz Mie theories, from past to future. *Atom Sprays* 2000;10(3–5):277–334.
- [3] Maheu B, Gouesbet G. A concise presentation of the generalized Lorenz–Mie theory for arbitrary location of a scatterer in an arbitrary incident profile. *J Opt* 1988;19:59–67.
- [4] Mishchenko M, Hovenier J. *Light scattering by nonspherical particles*. San Diego: Academic Press; 2000.
- [5] Bohren CF, Huffman DR. *Absorption and scattering of light by small particles*. New York: Wiley-Interscience Publications; 1998.
- [6] Van de Hulst HC. *Light scattering by small particles*. New York: Dover Publications; 1981.
- [7] Holoubek J. Optical transmission and light scattering of phase separation structures in polymer blends, Fourth international congress optical particle sizing, Nuremberg, 21–25 March, 1995. p. 387–96.
- [8] Girasole T, Rozé C, Maheu B, Gréhan G, Ménard J. Distances of visibility in a foggy atmosphere: comparisons between lighting installations by means of a Monte Carlo simulation. *Int J Light Res Tech* 1998;30(1):29–36.
- [9] Lavigne C, Roblin A, Outters V, Langlois S, Girasole T, Rozé C. Comparison of iterative and Monte Carlo methods for calculation of the aureole about a point source in the Earth's atmosphere. *Appl Opt* 1999;38(30):6237–46.
- [10] Prahl SA, Keijzer MR. Dosimetry of laser radiation in medicine and biology. A Monte Carlo model of light propagation in tissue, SPIE Insitute Series, vol IS 5 Publications, 1989. p. 102–11.